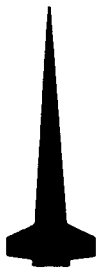


MI

AD



RSIC-676

# CONTACT DIFFUSION INTERACTION OF MATERIALS WITH CLADDING

by

A. A. Babad - Zakhryapina

Proceedings of the Symposium on Thermodynamics with Emphasis on Nuclear Materials and Atomic Transport in Solids. Organized by the International Atomic Energy Agency. Symposium held in Vienna 22-27 July 1965. Proceedings Series, 2, 153-180 (1966)

Translated from the Russian

May 1967

DISTRIBUTION OF THIS DOCUMENT IS UNLIMITED

## REDSTONE SCIENTIFIC INFORMATION CENTER REDSTONE ARSENAL, ALABAMA

JOINTLY SUPPORTED BY



U.S. ARMY MISSILE COMMAND



GEORGE C. MARSHALL SPACE FLIGHT CENTER

N67-34874

N67-34877

FACILITY FORM 602

(ACCESSION NUMBER)

(THRU)

42

(PAGES)

(CODE)

66-66158

(NASA CR OR TMX OR AD NUMBER)

23

(CATEGORY)

**Disclaimer**

The findings in this report are not to be construed as an official Department of the Army position unless so designated by other authorized documents.

**Disposition**

Destroy this report when it is no longer needed. Do not return it to the originator.

19 May 1967

RSIC-676

**CONTACT DIFFUSION INTERACTION OF MATERIALS  
WITH CLADDING**

by

A. A. Babad - Zakhryapina

Proceedings of the Symposium on Thermodynamics with Emphasis  
on Nuclear Materials and Atomic Transport in Solids. Organized  
by the International Atomic Energy Agency. Symposium held  
in Vienna 22-27 July 1965. Proceedings Series, 2, 153-180 (1966)

Translated from the Russian

**DISTRIBUTION OF THIS DOCUMENT IS UNLIMITED**

Translation Branch  
Redstone Scientific Information Center  
Research and Development Directorate  
U. S. Army Missile Command  
Redstone Arsenal, Alabama 35809

This published work discusses problems arising from diffusion interaction between materials and their claddings and the film of condensate formed on their surfaces. Since condensates practically always form on heated materials, the commencement of interaction is observed during the process of formation of the film. In this connection, the investigation of the characteristics of the diffusion interaction of the film with the materials should be divided into two stages: interaction during the process of the formation of the film and the interaction during the process of extended isothermal heating. Detailed results of two stages are presented in this work.

A characteristic of the first stage is the simultaneousness of the course of the two processes: condensation and diffusional transfer of the cladding material into a growing layer. The continuity of the condensate growth, as well as the law governing the growth of the layer itself, gives rise to the appearance of certain specific characteristics in the character of diffusion interaction (Section I).

The interaction of the film with the material during isothermal heating may occur at the expense of a decrease of the content of one of the components of the cladding material and not as a result of the interchange reaction. It is borne out that geometric correlations have a substantial influence on the character of diffusion process in such a system. This is shown by the example of contact diffusion of monocarbide of uranium with molybdenum and tungsten (Section II).

Besides these general questions concerning characteristics of diffusion interaction of deposited materials, investigation is also made of the correlation of the diffusional mobility of atoms with thermodynamic characteristics of materials.

In conclusion, a study is made of data concerning the diffusion of carbon in zirconium carbide (Section III).

**N67-34375**

## **I. CHARACTERISTICS OF DIFFUSION PROCESSES IN CONDENSATES, FORMED ON A HOT CLADDING**

by **A. A. Babad-Zakhryapina and L. Gert**

### **1. Introduction**

To create a well bonded layer of condensate with a cladding surface, it is common practice to utilize heating of the cladding during the process of condensation. During the course of the whole process, there occurs an inevitable diffusion interaction between the cladding

material and the condensate material, a characteristic of which is a diffusional penetration of the cladding material into the layer of condensate. On the other hand, the penetration of the condensate material into the cladding also, to a certain degree, has to be determined by the conditions of condensation.

The diffusion interaction between the cladding and the condensate may lead to a change in the conditions of condensation, i. e., a change in the character of dependence between the thickness of the layer and the time it takes to form, as well as have a substantial influence on the phase formation in the condensate layer. Regardless of the fact whether these phenomena are desirable or undesirable in the process of formation of the condensate layer, they have to be taken into account and a method, based on prior knowledge, has to be developed by which the phenomena can be evaluated quantitatively.

## 2. Unilateral Interaction of the Cladding Material with the Condensate Layer During the Process of the Layer Formation

For the solution of this problem, it is necessary to know the growth law of the condensate layer. Subsequently, two laws will be examined: linear, i. e., the growth of the layer with a constant speed and parabolic - with a variable velocity.

The simplest case, which is encountered in the investigation of the diffusion interaction of the cladding with the condensate, is the unilateral diffusion in the condensate layer. This case may be formulated in the following manner: on a cladding of material A at a temperature T, substance B is placed according to the law  $x = f(t)$  ( $t$ -time); it is necessary to determine the concentration of substance A (i. e.,  $c_A$ ) on the surface of the layer of condensate.

Here it will be assumed that the coefficient of diffusion A in B ( $D_{AB}$ ) is considerably greater than the coefficient of diffusion of B in A ( $D_{BA}$ ). For simplicity and ease of notation, let us consider that  $D_{BA} = 0$  and  $D_{AB} = D$ .

Boundary conditions for this problem have the form (Figure 1) on the interface cladding condensate.

$$c_A \frac{d\ell}{dt} = - D \left( \frac{\partial c}{\partial x} \right)_{c_A}, \quad c(x, t)_{x=0} = c_0$$

on the surface of the layer

$$c(x, t)_{x = \ell} = c_A, \text{ where } \ell = f(t).$$

From the general solution of the Fick equation for a unilateral source<sup>1</sup> and above boundary conditions for a case when  $\ell = 2b\sqrt{Dt}$ , we obtain:

$$c_A = \frac{c_0}{1 + F(b)} \quad (1)$$

where  $F(b) = \sqrt{\pi}b \exp b^2 \Psi(b)$ ,  $\Psi(b)$  - function of Gauss errors.

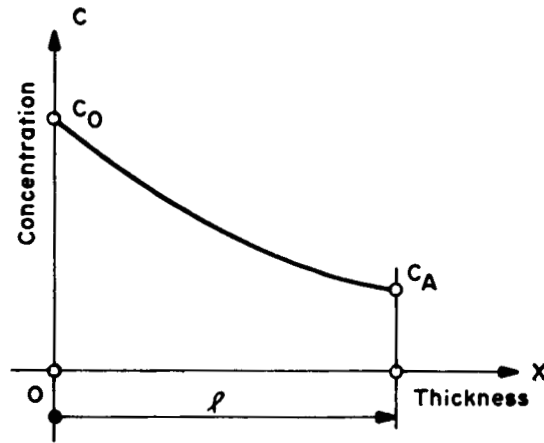


Figure 1. Diagram of the Distribution of Concentration in a Layer of Condensate in a Case of Unilateral Single Phase Diffusion

Under linear law of growth of layer, when  $\ell = kt$

$$c_A = \frac{c_0}{1 + F(k, t)} \quad (2)$$

where

$$F(k, t) = k \sqrt{\frac{\pi t}{D}} \exp - \frac{k^2 t}{4D} \Psi \left( \frac{\ell}{2\sqrt{Dt}} \right).$$

The expression, determining  $c_A$  under linear law of layer growth, is an approximation and may be utilized for calculations at low values of

k and t. An accurate solution of this problem may be obtained by the solution of the equation of material balance on the boundary of cladding condensate, where

$$- D \frac{\partial c}{\partial x} \Big|_{x=\ell} = c_A k, \quad (3)$$

bearing in mind that  $d\ell / dt = k$ .

Let us perform a substitution of variable  $k = \ell$ . Such a substitution is possible provided that

$$\frac{\partial c}{\partial t} \Big|_{\ell} = \frac{dc_A}{dt} .$$

We will prove that the latter equivalence is valid only in the case if  $\ell = kt$ . Differentiating Equation (3) according to  $\ell$  and comparing the obtained result with the Fick equation for point  $\ell$ , we obtain

$$c_A \frac{d}{d\ell} \left( \frac{d\ell}{dt} \right) = 0 .$$

As  $c_A \neq 0$  according to the problem, then  $(d/d\ell) (d\ell / dt) = 0$  which gives  $\ell = kt$ .

Bearing in mind that  $c(\ell, t) = c_A$  and  $- D (\partial c_A / \partial \ell) = c_A k$ , after transfer to variable "k", we obtain

$$c(x, t) = c_0 \exp \left( -\frac{kx}{D} \right) . \quad (4)$$

Let us prove that expression (4) satisfies Fick's equation and boundary conditions. For this purpose, it is expedient to go to another system of coordinates  $X = \ell - x$  (Figure 2). In the new system of coordinates, expression (4) will be written as

$$c(X, t) = c_0 \exp \left( \frac{kX - k^2 t}{D} \right) . \quad (5)$$

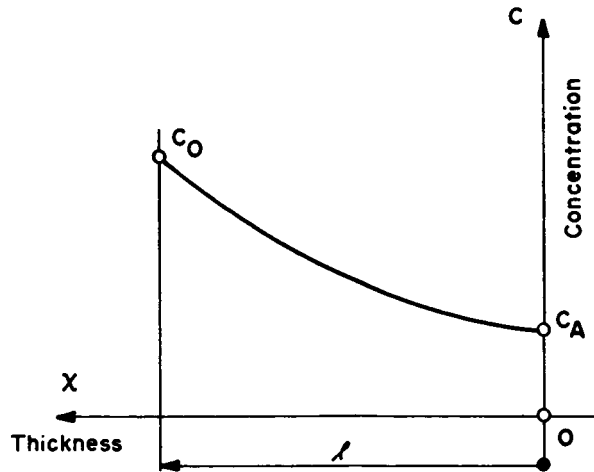


Figure 2. The Connection Between Systems of Coordinates Showing the Dependence of the Concentration of Cladding Material in the Condensate Layer on the Growth Rate Under the Linear Law for the Growth of the Condensate

By direct substitution, it is easy to be convinced that expression (5) satisfies both the Fick equation and boundary conditions.

From Equation (4), it follows that the distribution of the concentration in the layer of the condensate, growing according to linear law, is pseudo-stationary. The form of the concentration curve in this case is determined only by the relationship  $k/D$ .

With the increase of the growth rate, the concentration of layers at any one given point, and consequently on the surface, decreases. The same conclusion is arrived at by analysis of approximated correlation(2).

In any case of parabolic law of growth,  $c_A$  remains a constant independent of time while its value is determined only by parameter "b". The above obtained correlations (3) and (4) may be utilized for determination of coefficients of diffusion. The most suitable for this purpose is correlation (4). Conducting a linear interpolation of the concentration curve, which is permissible for lower values of  $kx/D$ , we obtain  $c(x, t) = c_0D/(D + kx)$ . In this relationship, magnitudes of "k" and "x" are easily determined experimentally. Thus, for computation of D, it is only necessary to know the concentration at any one given point along the thickness of the layer. In the case where, as a result of diffusion, solid solutions are formed and if the concentration dependence of the lattice parameter is known, then the concentration on the surface of the layer can be determined by X-rays.

Now let us examine a case where, as a result of diffusion, there is a possibility of formation of two phases in the growing layer: one with a large content of substance A (phase I) and another with a lesser content (phase II). The boundary conditions of such a problem appear as follows (Figure 3): at  $l = 0$   $c = c_0$ , at  $l = l_1$ , there is a constant range of the concentration  $c_{1,2} - c_{2,1}$  at  $l = l_2$   $c = c_A$ .

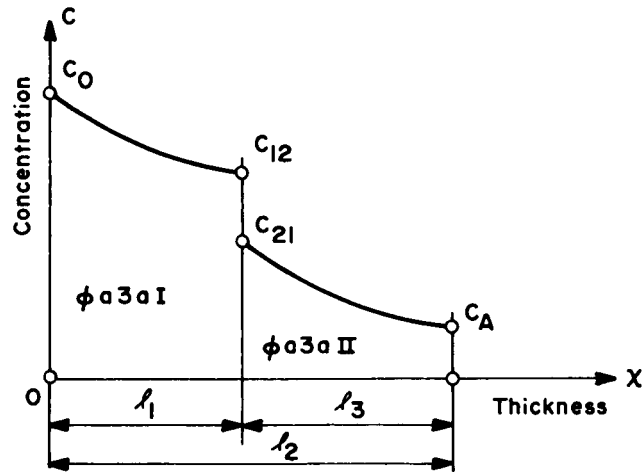


Figure 3. Diagram of the Distribution in the Condensate Layer in the Case of Two Phase Unilateral Diffusion

This problem may be solved in the same manner as the preceding one but with one difference, that the solution is actually conducted separately for ranges  $0 \leq x < l_1$  and  $l_1 < x \leq l_2$  ( $l_1$  and  $l_2$  are areas of existence of phases I and II) and is realizable as one single solution by means of the material balance condition on the boundary of the separation of phases. It is assumed that the movement of the boundary between phases or growth of phase I occurs according to the parabolic law  $x_1 = 2b_1\sqrt{D_1t}$ . For the parabolic law of the layer growth ( $x_2 = 2b_2\sqrt{D_2t}$ ), there may be obtained an equation connecting the value of the concentration with parameters  $b_1$  and  $b_2$ :

$$\frac{c_{2,1} - c_{1,2}}{c_0 - c_{1,2}} = \frac{c_{2,1}}{c_0 - c_{1,2}} \cdot \frac{F(b_1b_2)}{F(b_1\phi) [F(b_1b_2) + 1]} - \frac{1}{F(b_1)} .$$

This correlation permits the evaluation of the character of the dependence between  $b_1$  and  $b_2$ . In the context of the problem,  $b_2$  may vary within the limits  $b_1 \leq b_2 < \infty$ . At  $b_2 = b_1F(b_1b_2) = 0$  and

$\frac{c_0 - c_{1,2}}{c_{1,2}} = F(b_1)$ , i. e., on the growing surface a constant concentration  $c_{2,1}$  is maintained.

If  $b_2 \rightarrow \infty$ , then  $F(b_1 b_2) \rightarrow \infty$  and  $c_{2,1} - c_{1,2} = \frac{c_0 - c_{2,1}}{F(b)} - \frac{c_{1,2}}{F(b_1 \phi)}$ , this is equivalent to diffusion into semi-infinite space<sup>1</sup>. It is easy to demonstrate that  $b_1$  exists only in a certain definite range of values and decreases with the increase of  $b_2$ , reaching into limits of values, corresponding to a case of jet diffusion into semi-infinite space.

Under the linear law of growth of the layer in an analogous manner (such as that for a case under parabolic law), an approximated correlation may be obtained:

$$\frac{c_{2,1} - c_{1,2}}{c_0 - c_{1,2}} = \frac{c_{2,1}}{c_0 - c_{1,2}} \cdot \frac{F(ktb_1)}{F(b_1 \phi) [F(ktb_1) + 1]} - \frac{1}{F(b_1)}$$

where

$$F(ktb_1) = \sqrt{\pi} \sqrt{\frac{t}{D_2}} \left( kt - b_1 \sqrt{\frac{D_1}{t - t_0}} \right) \exp\left(\frac{k}{2} \sqrt{\frac{t}{D}}\right)^2 \Psi\left(-\frac{k}{2} \sqrt{\frac{t}{D_2}}\right),$$

$t_0$  - time,

upon conclusion of which phase II was formed in the layer. This correlation, just as for the case of one phase diffusion, may be utilized with small  $k$  and  $t$ . Its analysis shows that with the diminution of  $k$  and  $t$ , there occurs an increase of  $b_1$ . The application of a quasi-stationary method of computation for the linear growth law permits computation of the initial single phase diffusion. The solution in differential form for this case has the appearance as follows:

$$\left\{ \begin{aligned} D_2 c_{2,1} - D_2 c_A &= \frac{c_{2,1}}{2} (kt - \ell_1) \left( k - \frac{d\ell_1}{dt} \right) + \frac{dc_A}{dt} \cdot \frac{1}{2} (kt - \ell_1)^2 \\ &+ \frac{c_A}{2} (kt - \ell_1) \left( k - \frac{d\ell_1}{dt} \right) \frac{c_{2,1} - c_0}{2} \cdot \frac{d\ell_1}{dt} = \frac{c_0 - c_{2,1}}{\ell_1} D_2 \\ &+ \frac{c_A - c_{1,2}}{kt - \ell_1} D_1. \end{aligned} \right.$$

This system may be solved by any one of the well known methods of approximated solutions. As a result, it will be found that  $\ell_1 = \phi(t)$  and  $c_A = f(t)$ .

### 3. Interaction of the Condensate with the Cladding During the Process of the Layer Formation

As in the preceding paragraph, an assumption will be made that in the process of the layer formation of condensate, there occurs a unidirectional diffusion of the condensate material into the cladding.

Let us examine a case of parabolic law growth of the condensate and single phase diffusion (Figure 4).

At  $x_1 = 2b_1\sqrt{D_1t}$  and  $x_2 = 2b_2\sqrt{D_2t}$ , we obtain

$$\left\{ \begin{array}{l} \frac{c_B - c_1}{c_1} = \sqrt{\pi} b_1 \exp b_1^2 \left[ \Psi(b_1) + \Psi(b_2) \right] \\ \frac{c_B - c_1}{c' - c_B} = \sqrt{\pi} b_2 \exp b_2^2 \left[ \Psi(b_1) + \Psi(b_2) \right] \end{array} \right.$$

where  $c'$  is the concentration of B in the condensate material of composition  $A_m B_n$ ,

$c_B$  is the concentration of B on the surface of the condensate,

$c_1$  is the lowest concentration of B in the forming phase,

$c_0$  is the concentration of B on the separation boundary of the cladding and the layer of the condensate,

$x_2$  is the coordinate of the surface of the growing layer of the condensate,

$x_1$  is the coordinate of the concentration stagger  $c_1 - 0$  of the forming phase.

Estimation of the dependence  $c_B$  and  $b_1$  on  $b_2$  shows that an increase of  $b_2$  leads to a decrease of  $b_1$  and an increase in  $c_B$ . At  $b_2 \rightarrow \infty$ , the resulting expressions transform themselves into expressions describing diffusion from semi-infinite space<sup>1</sup>.

However, if the velocity of the input of the substance into the cladding is so insignificantly small that it is immediately absorbed, then the problem becomes considerably more complex. A variant of such a problem, namely, absorption of preliminarily accumulated layer, is investigated by Malkovich<sup>2</sup>.

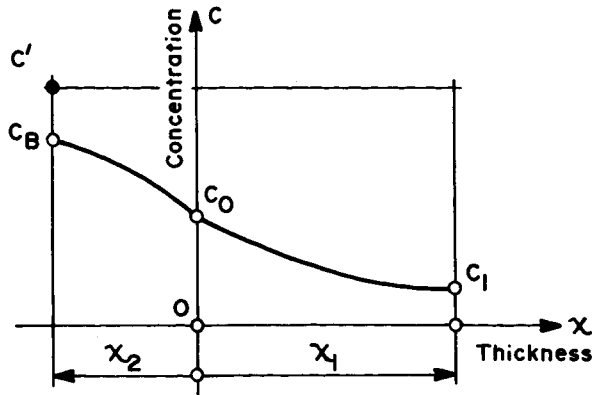


Figure 4. Diagram of the Distribution of Concentration During Unilateral Single Phase Diffusion of the Condensate Material into the Cladding

#### 4. Characteristics of Phase Formation in Condensate Layers Formed on a Hot Substrate

It has been shown above that under parabolic law of growth of the condensate, the concentration of the cladding material on the surface of the layer remains constant; however, in the case of linear law, it varies with the passage of time in the direction of diminutions. In Figure 5, both laws of growth are shown in general form. At point A, the tangential line to the parabola is parallel to the straight line, corresponding to the linear law growth of the layer. On sector OA, the rate of the layer growth is greater than in the case under linear law, while on sector AB it is smaller.

Let us juxtapose the characteristics of the layer growth of condensate  $c_A$  formed under parabolic and linear laws. With the thickness of the layer  $l = OF$  grown according to linear law, the concentration is greater on the surface. With the thickness  $OF < l \leq O\infty$ , the surface concentration will be smaller than  $c_A$ , i. e., the rate of the layer formation on this sector is greater than it is necessary for the support of concentration  $c_A$  on the surface. The ultimate thickness (limit) at which there shall occur a drop in concentration from  $c_0$  to  $c_A$  is  $l = O\infty$ . In a general case this will occur at  $OF < l < O\infty$  during time  $t_A < t < t_B$ .

It has been noted above that the highest rate of phase growth in the condensate is assured with the formation of the layer according to the parabolic law. However, in the case of formation of the phase during

diffusion into semi-infinite space, the phase growth occurs also according to parabolic law but with a lesser speed.

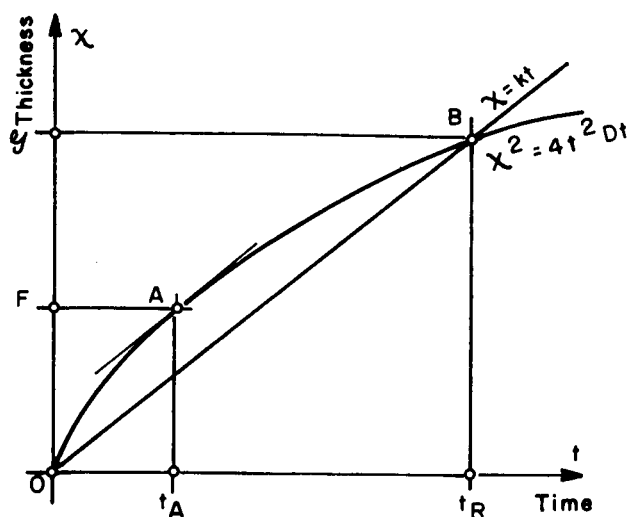


Figure 5. Diagram Illustrating Correlations Between Rates of Growth Under Parabolic and Linear Law at Equal Time

In Figure 6, two parabolas are shown corresponding to the growth of the phase in layer (1), formed according to parabolic law, and during diffusion into semi-infinite space (2).

With the growth of the phase in the layer formed according to linear law, it is possible to select such a rate of growth that in time  $t$ , the thickness of the phase in this layer will be lesser according to curve 2 in growth but greater according to curve 1, i. e.,  $l_2 < l < l_1$ .

Thus, under the linear growth law of the layer, the picture of the distribution of phases is more extended than in the case of diffusion into semi-infinite space. This characteristic of phase formation under the linear growth law permits the growing of phases with a narrow area of homogeneity up to a certain noticeable thickness.

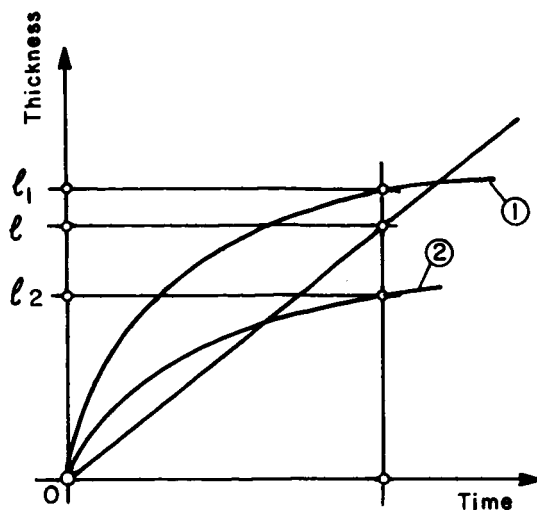


Figure 6. Diagram, Illustrating Correlations Between the Thickness of the Phases in the Case of the Growth of the Phase in the Layer, Formed According to Parabolic Law (2), Upon Diffusion Into Semi-infinite Space (1) and in a Layer Formed According to Linear Law

N67-34376

## II. DIFFUSION OF CARBON FROM CARBIDE OF URANIUM INTO MOLYBDENUM AND TUNGSTEN

by V. S. Eremeyev, A. S. Panov, B. F. Ushakov,  
and Ye. V. Fiveiskii

### 1. Introduction

In connection with the search for new high temperature construction materials during the last two decades, many works have appeared on the investigation of the characteristics of carbides of transmutable metals<sup>3, 4, 5</sup>. Specifically, attention was focussed on the problems of diffusional mobility of carbon in carbides of transition metals<sup>6, 7, 8, 9</sup> as well as the problems of contact interaction of carbides with metals<sup>10, 11, 12, 13</sup>.

In research on contact interaction of carbides with metals having a high melting point, two cases can arise. In the first case, an exchange reaction occurs of the type:



In the second case, the cause of the formation of the carbide layer on the metal in contact is the migration of atoms of carbide into the metal. This migration is realized either as a consequence of surplus content of carbon in comparison with stoichiometry or because of the fact that carbide passes to the lower limit of the homogeneity area. With this, the following reaction occurs:



where  $C_y$  is the lower limit of the area of homogeneity of carbide  $Me_I C_{y+x}$ .

In principle, the reaction of the first type may be accompanied by the reaction of the second type. However, cases may occur when, in spite of the fact that the reaction of the first type is thermodynamically impossible, the contact interaction does take place. Systems UC - Mo or UC - W may serve as an example of this. Probably only by means of the reaction of the second type is it possible to explain the contact interaction of stoichiometric monocarbide of uranium with molybdenum and tungsten<sup>14,15</sup>.

The relatively limited available data from literature on the subject of the kinetics of solid phase reactions in such systems are often contradictory. Therefore, the study of contact interaction in system  $Me_I C - Me_{II}$ , where the reaction of the type Equation (6) takes place, presents an unusual interest.

In the current work, equations corresponding to the reaction of the type Equation (6) are solved, and discussion is presented on the influence of the carbon content on the kinetics of the process. For the purpose of substantiating the computed values, a study is made of the contact interaction of the carbide of uranium with molybdenum and tungsten at 1000°C.

## 2. The Solution of the Diffusion Equation for a Case of Migration of Carbon From Carbide into Metal

The solution of a system of equations, describing the kinetics of solid phase reactions, often becomes complicated. Specifically, when the limiting stages are diffusion processes and the kinetic factors on the boundaries of separation of phases may be ignored, the finding of solutions is considerably facilitated.

Let us examine the contact interaction in system  $Me_I C - Me_{II}$ . Let us limit ourselves by a case, when the kinetics of the growth of the

forming layers is determined by the migration of carbon from the carbide into the metal, and furthermore the reaction takes place according to the type Equation (6). The proposed scheme is applicable for those systems of  $Me_I C - Me_{II}$  when  $Me_I C$  is thermodynamically more stable than  $Me_{II} C$ , while the growth of the carbide layer on  $Me_{II}$  is realized at the expense of excessive carbon in the carbide of  $Me_I C$  in comparison with the concentration of carbon corresponding to the lower limit of the area of homogeneity of  $Me_I C$ .

Figure 7 schematically illustrates the distribution of the concentration of carbon in the process of jet reactive diffusion of carbon from carbide into the metal at moment of time  $t$ .

In this connection, the following designations are introduced.  $C_{12}$  and  $C_{22}$  are the concentrations of carbon on the boundaries of the forming carbide phase,  $C_{22}$  is the concentration of carbon corresponding to the lower limit of the area of homogeneity of the forming carbide, and  $C_{12}$  may be found after the solution.  $C_{33}$  corresponds to the maximum solubility of carbon in the metal and  $\epsilon$  is the thickness of the forming phase.

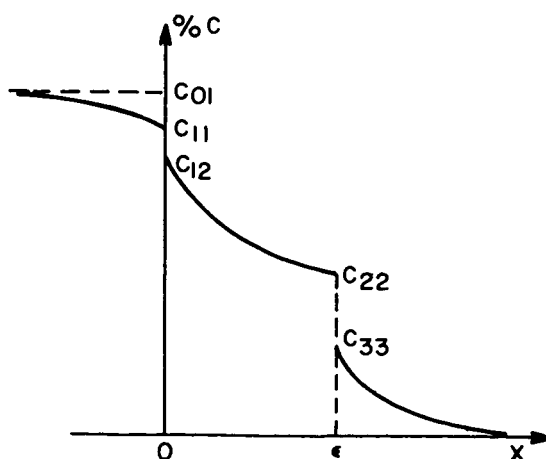


Figure 7. The Distribution of the Concentration of Carbon in the Process of Its Jet Diffusion from Carbide into the Contacted Metal at Moment of Time  $t$

Let us examine two cases:

- 1) Diffusion of carbon from a semi-infinite body
- 2) Diffusion from a finite body.

The first case belongs to the well known class of Stefan problems with parabolic law of growth<sup>9</sup>.

a. The Case of the Semi-infinite Body

For the three diverse phases  $Me_I C$  (phase 1), of the forming carbides  $Me_{II} C$  (phase 2) and the contacted metal (phase 3), let us put down the diffusion equation.

$$\frac{\partial C_i}{\partial t} = D_i \frac{\partial^2 C_i}{\partial x^2} \quad (1)$$

$$i = 1, 2, 3,$$

where index 1 corresponds to phase  $Me_I C$ ,

index 2 is the forming carbide  $Me_{II} C$ ,

index 3 is the contacted metal,

$D_1$  is the coefficient of diffusion of carbon in  $Me_I C$ ,

$D_2$  is the coefficient of diffusion of carbon in  $Me_{II} C$ ,

$D_3$  is the coefficient of diffusion of carbon in metal.

Boundary and initial conditions have the form:

$$\begin{aligned} C_1(x, 0) &= C_{01}, & x &\leq 0 \\ C_1(0, t) &= C_{11}, \\ C_2(\epsilon, t) &= C_{22}, \\ C_3(\epsilon, t) &= C_{33}, \\ C_3(\infty, t) &= 0. \end{aligned} \quad (2)$$

The conditions of the mass balance on the separation boundaries at  $x = 0$  and  $x = \epsilon$  are written down as follows:

$$D_1 \left( \frac{\partial C_1}{\partial x} \right)_{x=0} = D_2 \left( \frac{\partial C_2}{\partial x} \right)_{x=0} \quad (3.1)$$

$$- D_2 \left( \frac{\partial C_2}{\partial x} \right)_{x=\epsilon(t)} = \frac{d\epsilon}{dt} (C_{22} - C_{33}) - D_3 \left( \frac{\partial C_3}{\partial x} \right)_{x=\epsilon(t)}. \quad (3.2)$$

The separation boundary of phases at  $x = \epsilon$  is transposed according to the law

$$\epsilon = 2a\sqrt{D_2t} . \quad (4)$$

Equation (4) determines the position of the phase boundary between the forming carbide and the metal in contact. The constant "a" is the means for the solution of Equation (1) with fulfillment of conditions (2) and (3).

Omitting intervening insertions, we will set down the equation from which it is possible to determine "a":

$$\frac{C_{01} - C_{11}}{C_{22}} \sqrt{\frac{D_1}{\pi D_2}} \cdot \frac{1}{a} = \exp a^2 + \frac{C_{33}}{a C_{22}} \sqrt{\frac{D_3}{\pi D_2}} \cdot \frac{\exp a^2 \left(1 - \frac{D_2}{D_3}\right)}{\left[1 - \operatorname{erf} \left(a \sqrt{\frac{D_2}{D_3}}\right)\right]} \quad (5)$$

where  $\operatorname{erf}(z) = \frac{2}{\sqrt{\pi}} \int_0^z \exp -z^2 dz$ .

If  $D_3 < D_2$  and  $C_{33} \ll C_{22}$ , then the expression (5) may be simplified:

$$\frac{C_{01} - C_{11}}{C_{22}} \sqrt{\frac{D_1}{\pi D_2}} = a \exp a^2 . \quad (6)$$

Equalities (4) and (6) determine the speed of the formation of the carbide phase if the dimensions of the contacted carbide satisfy the conditions of the semi-infinite body.

Let us note, however, that in case of fulfillment of equality (6), the concentration of  $C_{12}$  in the forming carbide on the boundary of  $x = 0$  is determined by equation:

$$C_{12} = C_{22} - (C_{01} - C_{11}) \sqrt{\frac{D_1}{D_2}} \operatorname{erf}(a) . \quad (7)$$

If it turns out that  $C_{12}$  is higher than the concentration of carbon  $C_{12}^*$ , corresponding to the upper limit of the area of homogeneity in the forming carbide, then in order to determine the parameter of "a" instead of Equation (6), the following expression has to be used:

$$\frac{C_{12}^* - C_{22}}{C_{22}} = a \sqrt{\pi} \operatorname{erf} a \exp a^2 . \quad (8)$$

Equality (8) follows from the assumption that on the boundary  $\text{Me}_I C - \text{Me}_{II} C$ , the maximum possible concentration of  $C_{12}^*$  is maintained

while the kinetics of the growth of the layer are subject to parabolic law.

The issue of formula (8) is given in work by Gertsriken and Dexter<sup>16</sup>.

b. The Case of the Finite Body

Let the diffusion of carbon occur from a plate of  $\ell$  thickness. The initial concentration of carbon in the plate is equal to  $C_{01}$ . In the process of diffusion on the boundary of the plate at  $x = 0$  and  $x = \ell$ , a concentration of carbon equal to  $C_{11}$  is maintained. Then utilizing the known solution for this case<sup>17</sup>, it is possible to demonstrate that the flow of the diffusion component on the boundary  $x = 0$  and  $x = \ell$ , is equal to:

$$p = \frac{4 D_1}{\ell} (C_{01} - C_{11}) \sum_{m=0}^{\infty} \exp - \frac{D_1 (2m + 1)^2 \pi^2 t}{\ell^2} .$$

For simplification of the problem, let us examine a case when the flow of carbon, diffusing from the forming carbide into the metal, is insignificant and has practically no influence on the speed of the formation of the carbide phase of the metal.

We will find the speed of the growth of the carbide phase on the metal if on the boundary of the example at  $x = 0$ , a flow is unleashed, determined by Equation (7) while at  $x = \epsilon$  the concentration is maintained constant and is equal to  $C_{22}$ . In a general form, this problem is solved in other work<sup>18</sup>. Utilizing this solution as applicable to our case, we may set down:

$$\sum_{k=0}^{\infty} \frac{1}{D_2^k (2k + 1)} \left[ \frac{d}{d t^{(k + 1)}} \left[ \epsilon^{2k + 1} (t) \right] \right] = \frac{4 D_1 (C_{01} - C_{11})}{\ell C_{22}} \sum_{m=0}^{\infty} \exp - \frac{D_1 (2m + 1)^2 \pi^2 t}{\ell^2} .$$

Here the designations are the same, as those in point (1).

First let us find the solution (8) in the assumption that in the right side we may be limited to one first member, corresponding to  $m = 0$ . This is assumed valid at

$$\frac{D_1 \pi^2 t}{\ell} \gg 1 .$$

The solution we seek is in the form of:

$$\epsilon = A_0 - B_0 \exp - \frac{D_1 \pi^2 t}{\ell^2} \quad . \quad (9)$$

After transformation, the left side in Equation (8), taking into consideration Equation (9), is written as follows:

$$\sum_{n=1,2,\dots}^{\infty} e^{-2n\alpha t} \sum_{k=n,n+1,\dots}^{\infty} \frac{(2k+1)\dots(2k-2n+3)A_0^{2k-2n+2} B_0^{2n-1} [(2n-1)^\alpha]^{k+1}}{D_2^k (2k+1) | (2n) | (-1)^{k+1}}$$

$$+ \sum_{n=1,2,\dots}^{\infty} e^{-2(2n-1)\alpha t} \sum_{k=n-1,n,\dots}^{\infty} \frac{(2k+1)\dots(2k-2n+3)A_0^{2k-2n+2} B_0^{2n-1} [(2n-1)^\alpha]^{k+1}}{D_2^k (2k+1) | (2n-1) | (-1)^k} \quad ,$$

where  $\alpha = \frac{D_1 \pi^2}{\ell^2}$  .

After substitution of sensible values  $\ell = 0.4$  cm,  $D_1 \sim D_2 \sim 10^{-10}$  cm<sup>2</sup>/sec,  $A_0 \sim B_0 \sim 0.01 - 0.03$ , we obtain the information that the members of the row recede and disappear very quickly, and therefore it is possible with great accuracy to get by only with the first member ( $n = 1, k = 0$ ), which is equivalent to:

$$\frac{B_0 D_1 \pi^2}{\ell^2} \exp - \frac{D_1 \pi^2 t}{\ell^2} \quad .$$

From this we find:

$$B_0 = \frac{4 \ell}{\pi^2} \frac{(C_{01} - C_{11})}{C_{22}} \quad . \quad (11)$$

For determination of  $A_0$ , we will make use of the obvious equality

$$\epsilon_{t=\infty} = \frac{\ell (C_{01} - C_{11})}{2C_{22}} \quad . \quad (12)$$

Finally, we set down

$$\epsilon = \frac{\ell (C_{01} - C_{11})}{2C_{22}} \left( 1 - \frac{\ell}{\pi^2} \exp - \frac{D_1 \pi^2 t}{\ell^2} \right) \quad . \quad (13)$$

The obtained solutions (4) and (13) complement one another. Solution (4) is valid at low temperatures and small "t". Solution (13) is valid at high temperatures and high "t". It is considerably more suitable to conduct the investigation of the conditions of applicability of one form or another not in general, but with a specific system.

Let us apply the above expressions for determination of layers of interaction in systems UC - Mo and UC - W. To bring the problem to the stage of designated layers, it is necessary to know the coefficients of diffusion of carbon in the carbides of uranium, molybdenum, and tungsten as well as in molybdenum and tungsten.

### 3. Review of Data on Diffusion Constants in Molybdenum, Tungsten, and Carbides Mo<sub>2</sub>C, W<sub>2</sub>C, and UC

Data on diffusion mobility of carbon in carbides of uranium, molybdenum, tungsten as well as in tungsten are collected in Table I.

The coefficient of diffusion of carbon in the carbide of uranium at 1000°C is obtained by means of extrapolation of data given by Samsonov, Strashinskaya, and Shiller<sup>10</sup>.

The admissibility of such extrapolation is substantiated by experimental results<sup>20</sup> carried out in the temperature range interval 800° - 1100°C.

Literature contains no reliable data on the study of diffusional mobility of carbon in Mo<sub>2</sub>C and Mo at 1000° - 1400°.

The results of work by Samsonov and Epik<sup>7</sup> concern much higher temperatures.

Extrapolation of these data for 1000°C may lead to great error.

Work by Takenchi, Homma, and Sato<sup>20</sup> describes the measurement of diffusional mobility of carbon in molybdenum with application of isotope C<sup>14</sup>. The authors of this work noted as well the fact of the formation of carbide of molybdenum during diffusional holding time, which lessens significantly the value of their results. The study of the diffusional mobility of carbon in molybdenum presents great difficulties in view of its low solubility in molybdenum.

The experiments conducted by us according to the methods described by Gel'D and Lubimov<sup>6</sup> have shown that at 1000°C the coefficient of diffusion of carbon in molybdenum is no greater than  $10^{-12}$  cm<sup>2</sup>/sec. Also,

taking into consideration the insignificant solubility of carbon in molybdenum (about 0.02 weight percent C)<sup>20</sup>, expression (5) for computation of "a" may be replaced by Equation (6). The same applies to tungsten.

For determination of coefficients of the diffusion of carbon in Mo<sub>2</sub>C, the following work has been performed. Samples were prepared from melted down molybdenum (99.9 percent pure) and placed in contact at 1000°C with high purity graphite.

The thickness of the Mo<sub>2</sub>C layer formed on molybdenum was determined on a micrometric-durometer PMT-3 as an average for 100 measurements. The results of the measurements are compiled in Table II.

A constant concentration of C<sub>12</sub><sup>\*</sup> was maintained on the surface of molybdenum samples used in the conducted experiments. For this reason, Equations (4) and (8) may be used for computation of the coefficient of diffusion. The method employed for such computation is given by Gertsriken and Dexter<sup>16</sup>. The average value of the coefficient of diffusion of carbon in Mo<sub>2</sub>C after adjusting the experimental data (Table II) turned out to be equal to  $2 \cdot 10^{-11}$  cm<sup>2</sup>/sec at 1000°. During computation<sup>5</sup>, it was accepted that C<sub>12</sub><sup>\*</sup> = 0.536 g/cm<sup>3</sup> and C<sub>22</sub> = 0.491 g/cm<sup>3</sup>.

#### 4. Computation of the Thickness of Carbide Layers Formed on Molybdenum and Tungsten on Contact with Carbide of Uranium

For computation of the thickness of forming carbide layers on molybdenum and tungsten after contact with carbide of uranium, formula (4) is utilized. Coefficient "a" is found from Equation (6). Equation (6), as has been shown above, is valid, provided the flow of carbon under conditions (3.2)  $D_3 \left( \frac{\partial C_3}{\partial x} \right)_{x = \epsilon(t)}$  can be ignored.

In our case, due to the low solubility of carbon in molybdenum and tungsten, this condition is fulfilled of which one may find substantiation using the following initial data:

$$\begin{aligned} C_{11} &= 0.6188 \text{ g/cm}^3 \text{ at } 1000^\circ \text{C}^{12} \\ C_{22} &= 0.4914 \text{ g/cm}^3 \text{ for Mo}_2\text{C}^5 \\ C_{22} &= 0.4671 \text{ g/cm}^3 \text{ for W}_2\text{C}^5 \\ C_{23} &= 0.001 \text{ g/cm}^3 \text{ for Mo}^{22}. \end{aligned}$$

Table I. Diffusion Constants in the Case of Diffusion of Carbon into UC, Mo<sub>2</sub>C, W<sub>2</sub>C, and W

Diffusion Medium	Method	Temperature Interval, °C	D <sub>0</sub> cm <sup>2</sup> /sec	kcal/mol	D at 1000°C	Authors
UC	C <sup>14</sup>	1470 - 2270	2 · 10 <sup>-2</sup>	50	5.92 · 10 <sup>-11</sup>	9
Mo <sub>2</sub> C	M	1400 - 1800	780	83	5.42 · 10 <sup>-12</sup>	7
W <sub>2</sub> C	M	1525 - 1850	25,000	112	1.97 · 10 <sup>-15</sup>	8
W	C <sup>14</sup>	1230 - 2014	1.6 · 10 <sup>-6</sup>	50	4.74 · 10 <sup>-15</sup>	19
Mo <sub>2</sub> C	M	1000 - 1400			2.0 · 10 <sup>-11</sup>	Published Works

- Notes: 1) C<sup>14</sup> - Method with application of radioactive isotope C<sup>14</sup>.  
 2) M - Metallographic determination of the coefficient of diffusion along the thickness of the forming layer.

Table II. Thickness in Microns of the Mo<sub>2</sub>C Layer Forming on Molybdenum After Contact with Graphite

Temperature (°C)	Time (hr)		
	100	250	500
1000	8 ± 2	19 ± 2	28 ± 3

To elucidate the influence of carbon content in the monocarbide of uranium on growth rate of forming layers, let us select three values of concentration of carbon C<sub>01</sub> in monocarbide equal to 0.624 g/cm<sup>3</sup>, 0.650 g/cm<sup>3</sup>, and 0.676 g/cm<sup>3</sup> which corresponds to 4.8, 5.0, and 5.2 of weight in percent.

We assume the density of the carbide of uranium to be equal to 13 g/cm<sup>3</sup>. The values of the coefficients of diffusion are cited in Table I.

The computed values of unknown constant "a" by means of the solution of the transcendental Equation (6) are cited in Table III.

The estimate of the concentration of carbon in the carbide of molybdenum at x = 0 according to Equation (7) shows that C<sub>12</sub> < C<sub>12</sub><sup>\*</sup> at 1000°C where C<sub>12</sub><sup>\*</sup> corresponds to the upper limit of the homogeneity range of Mo<sub>2</sub>C. Therefore, it is necessary to utilize expressions (4) and (6) in the computation of the forming layer during the initial period. In the case of tungsten, it turned out that C<sub>12</sub> is greater than C<sub>12</sub><sup>\*</sup> and equal to

0.55 g/cm<sup>3</sup> according to Samsonov<sup>5</sup>. Therefore, for tungsten, constant "a" is found from Equation (8). It is uniform for all compositions of the carbide of uranium 0.3.

Table III. Computed Values of Constant "a"

Diffusion Pairs	Temperature (°C)	Carbon Content in Monocarbide of Uranium, Percent of Weight		
		5.2	5.0	4.8
UC-Mo	1000	0.112	0.0612	0.0101
UC-W	1000	1.452	1.277	0.683

Let us cite the final form of dependence of thicknesses of formed layers on time:

$$\begin{aligned} \epsilon &= 9.1 \cdot 10^{-4} \sqrt{t} \text{ for UC(4.8 percent C) - Mo} \\ \epsilon &= 5.5 \cdot 10^{-3} \sqrt{t} \text{ for UC(5.0 percent C) - Mo} \\ \epsilon &= 1.0 \cdot 10^{-2} \sqrt{t} \text{ for UC(5.2 percent C) - Mo} \\ \epsilon &= 2.7 \cdot 10^{-4} \sqrt{t} \text{ for UC(4.8 - 5.2 percent C) - W} \end{aligned}$$

t in sec,  $\epsilon$  in  $\mu$ .

The solution of the equation of diffusion for a body of finite dimensions (Equation (13)), as has been noted above, is valid for extended times and high temperatures as well as with small thicknesses of  $l$ . In the investigated case at  $l = 0.4$  cm, the parabolic law of growth should be replaced by the law determined by formula (13) after  $10^5$  hours. In this manner at a temperature of  $1000^\circ\text{C}$  in the wide time interval, the finite dimensions of the body may be ignored and the parabolic law of growth utilized. But, however, with high temperatures and thicknesses of samples about 0.2 - 0.1 cm, it is necessary to use formula (13), i. e., to take into consideration the dimensions of the body already after 10 - 100 hours.

##### 5. Comparison of Computed and Experimentally Obtained Values of Thicknesses of Formed Carbide Layers on Molybdenum and Tungsten

With the aim of checking out the above presented computations, a task was set afoot to study experimentally the contact interaction of tungsten and molybdenum with the monocarbide of uranium. Samples of molybdenum and tungsten 09 mm and a height of 2 mm were cut from

forged rods obtained by the method of powder metallurgy. The purity of the metals was 99.9 percent. The carbide samples of the two substances (Table IV) 09 mm and h 4 mm were obtained by the powdered metallurgy metal. The density of the carbide samples was 12.6 - 12.7 g/cm<sup>3</sup>.

Table IV. Chemical Composition of Uranium Carbide (Weight Percent)

No. of Parties	U	C <sub>Total</sub>	C <sub>Free</sub>	N	O
1	95	4.7 - 4.9	0.1	0.005	0.15
2	94.8	5.0 - 5.2	0.1	0.005	0.15

The carbide and metallic samples were polished and placed sequentially into molybdenum containers.

The grooved connection of the cover of the container with the container assured a reliable contact. The diffusion annealing was conducted in a vacuum stove with a molybdenum heater in a vacuum  $4 \cdot 10^{-4}$  mm of mercury column at 1000°C up to 2500 hours. The accuracy of the temperature measurement was  $\pm 20^\circ\text{C}$ . After annealing, the samples from tungsten and molybdenum were investigated rontgenographically, metallographically, and radiometrically by measurement of  $\alpha$ -activity. Diffusional pairs were used for computation because they possessed satisfactory linkage. The experiments were duplicated.

The penetration of uranium into the contacted samples was insignificant for all investigated compositions. Along the layer, radiometric analysis did not uncover traces of uranium at a depth of 20  $\mu$  after diffusional annealing during 2500 hours. Therefore, it may be considered that the processes of mass transfer in the first approximation are determined by the diffusion of carbon.

On the surface of metallic samples after diffusional annealing, the layers of the resulting interaction were determined and measured metallographically.

The thickness of the layers is presented in Table V.

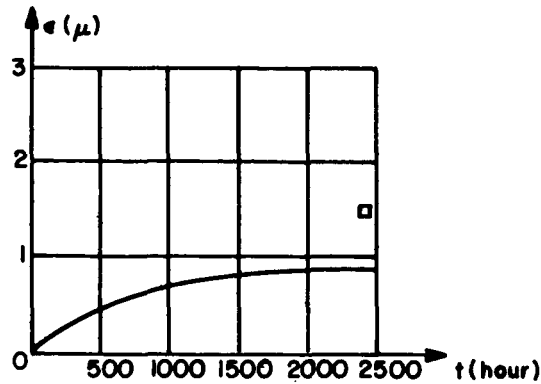


Figure 8. The Computed and Experimentally Obtained Values of the Thickness of the Formed Carbide Layers on Molybdenum After Its Contact with Carbide of Uranium at  $1000^{\circ}\text{C}$ . Curve 1, Obtained by Computation, Corresponds 5.2 Weight Percent C; Curve 2, 5.0 Weight Percent C; and Curve 3, 4.8 Weight Percent C in Carbide of Uranium.

Author's results:  $5.0 \div 5.2$  Weight Percent C in UC

$4.7 \div 4.9$  Weight Percent C in UC

Data from literature:  $\times 5.1$  Weight Percent C in UC<sup>9</sup>

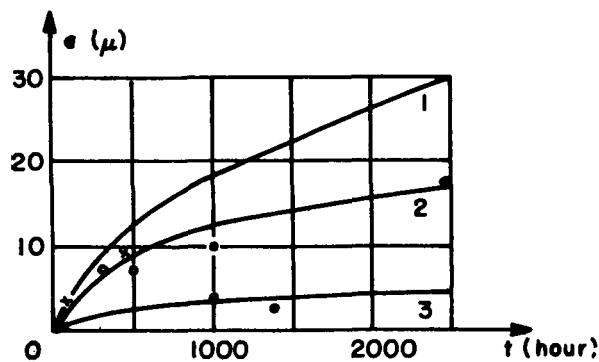


Figure 9. Computed and Experimentally Found Values of Thicknesses of Formed Carbide Layers on Tungsten After Its Contact with Carbide of Uranium at  $1000^{\circ}\text{C}$ . Curve 1 Corresponds 4.8 - 5.2 Weight Percent in UC.

Author's results: 5.0 - 5.2 Weight Percent C in UC.

Table V. Results of Interaction of Molybdenum and Tungsten with Carbide of Uranium at 1000°C

No. of Parties	Time (hr)	Thickness of Interaction Microns	
		Mo	W
1 (4.7 - 4.9 wt %)	1300	2 - 3	0.5
2 (5.0 - 5.2 wt %)	250	5	0.5
	500	8	0.5
	1000	10	0.5
	2500	+ 17	1 ÷ 2

Rontgen analysis has shown that the formed layers correspond to  $\text{Mo}_2\text{C}$  for molybdenum and  $\text{WC}$ ,  $\text{W}_2\text{C}$  for tungsten. In tungsten, in all cases X-ray analysis has shown the presence of phases  $\text{WC}$  and  $\text{W}_2\text{C}$ . As long as the sensitivity of the metallurgical method is not greater than  $0.5 \div 1$  micron, (then) the layers of carbides of tungsten were not noticed after extended contact of 250, 500, and 1000 hours with UC (5.0 - 5.2 weight percent) and 1300 hours with UC(4.7 - 4.9 weight percent).

Experimental data are presented in Table V together with computed values in Figures 8 and 9. In these very diagrams are also presented the results of work by Katz<sup>11</sup>. The computed and experimental values are in excellent agreement. Therefore, the proposed diffusional diagram of contact interaction is fulfilled, at least at 1000°C.

## 6. Conclusions

- 1) An equation for diffusion is solved which corresponds to the migration of carbon from carbide into the metal in contact with subsequent formation of carbide layer.
- 2) The interaction of carbide of uranium with molybdenum and tungsten at 1000°C up to 2500 hours has been experimentally investigated.
- 3) The computed values of the magnitudes of the forming layers are in satisfactory agreement with those arrived at experimentally.

### III. RESEARCH INTO THE DIFFUSION OF CARBON INTO ZIRCONIUM AND ZIRCONIUM CARBIDE

by R. A. Andrievskii, V. N. Zagryazkin,  
and G. Ya. Meshcheryakov

Information on the diffusional mobility of carbon in zirconium and its carbide is very limited. Babikov and Gruzin<sup>23</sup>, studying the electro-transfer of carbon into zirconium at 900°- 1200°C, have evaluated the numbers (numerical values) of the transfer. The determination of effective charge was not possible due to the absence of data on diffusion. In the work of Samsonov and his colleagues<sup>7</sup>, the diffusional saturation of zirconium by carbon was investigated, and certain energy parameters of interaction were evaluated. As far as it is known, these works force the only information on the diffusional mobility of carbon in zirconium and carbide of zirconium.

The samples of iodide zirconium and carbide of zirconium used by us in our work had the dimensions 10 - 12 mm and h 8 - 10 mm.

The latter sample was prepared by means of hot pressing at 2200°C under pressure of about 200 kg/cm<sup>2</sup> with a subsequent two hour annealing under the same temperature for homonization. The porousness of the samples did not exceed 5 percent; the composition of bonded carbon was 11.2 percent, which corresponds to the formula ZrC<sub>0.96</sub>; the quantity of free carbon was 0.65 percent, zirconium - 88.0; the lattice parameter - 4.697 Å. The iodide zirconium contained (weight percent) 0.01 C; 0.035 N; 0.11 O; 0.22 Fe; and 0.015 Hf. The quantity of the other admixtures was less than 0.005 weight percent.

The radioactive carbon C<sup>14</sup> was smeared in a thin layer on thoroughly polished bars of samples in the form of an emulsion in glycerine (specific gravity 30 microcurie/g). The samples were annealed by pairs in a graphite container which assured a tight contact of "active surfaces". The zirconium was annealed in a vacuum 10<sup>-4</sup> - 10<sup>-5</sup> Torr at 1100° - 1600°C and the carbide of zirconium was annealed in refined helium at 1600° - 2100°C. The temperature was measured by thermocouples Pt + 10 percent Rh/Pt and W + 5 percent Re/W + 20 percent Re with an accuracy ±20°C. After annealing, the samples were separated and a layer radiometric analysis was performed with construction of dependency  $\lg \mathcal{I} = f(x^2)$ , where  $\mathcal{I}$  is the intensity,  $\beta$  is the numbering (score), and  $x$  is the distance. In all cases, these dependencies had a linear character which evidenced adherence to conditions of diffusion from a thin layer (Figure 10). However, for zirconium (the initial one), two points sometimes do not fall on linear dependencies  $\lg \mathcal{I} - x^2$ , but microscopic and microdurometric investigations did not show formation of a carbide

phase. The coefficients of diffusion  $D$  were computed according to a well known formula:

$$D = \frac{0.1086}{\tau \tan \alpha} ,$$

where  $\tau$  is the annealing time and  $\tan \alpha$  is the tangent of the angle of incline of the straight (direct) line in coordinates  $\lg \rho - x^2$ . The method of the least squares was used for calculation of data.

Tables VI and VII and Figure 11 show the values of the coefficients of diffusion of carbon in zirconium and the carbide of zirconium. All values are averages from 3 - 4 measurements. For the diffusion of carbon in the carbide of zirconium, another method was also used. It consisted of the application of the carbide of zirconium containing radioactive carbon-14. The thickness of such a sample was 6 - 8 mm. Computation was conducted according to the well known formula for a case of diffusion from a constant source into infinite space. Both methods lead to very similar results. The difference in values of  $D$  fell well into the margin of error of the experiment. The maximal error in the determination of the coefficient of diffusion and energy of activation in our case consisted of about 20 and 4 percent, respectively.

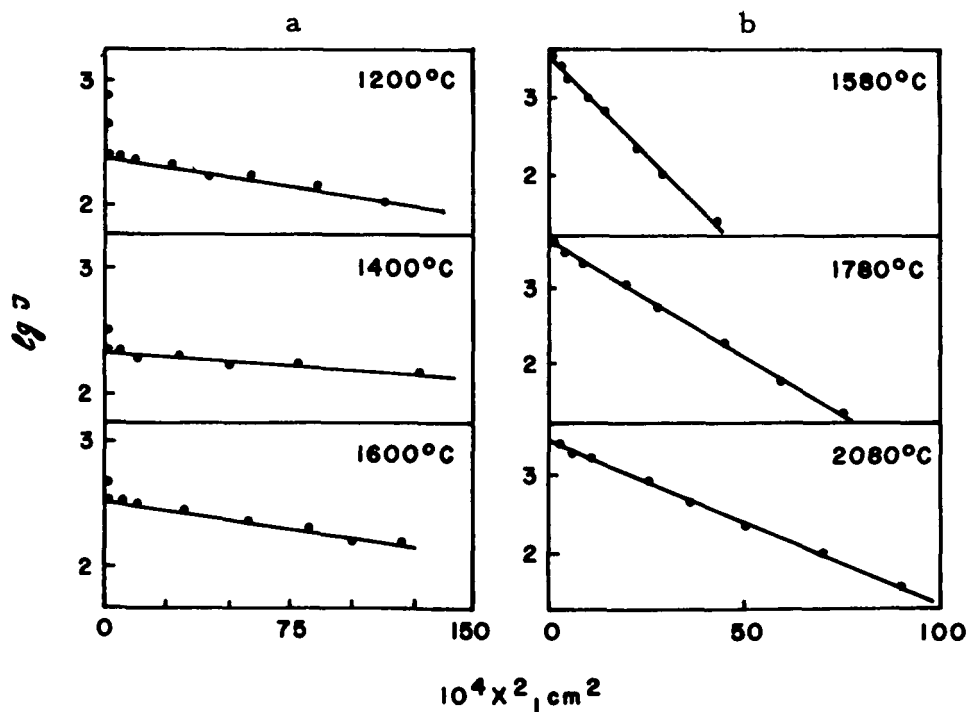


Figure 10. Results of Layer Radiometric Analysis in Coordinates  $\lg \rho - x^2$ : a - Zirconium; b - Carbide of Zirconium

The temperature dependencies of D, obtained with the help of the method of least squares, has the form

$$D_{c \rightarrow Zr} = 3.6 \cdot 10^{-2} \cdot \exp(-34,200) RT/cm^2/sec \quad (1)$$

$$D_{c \rightarrow ZrC_{0.96}} = 3.3 \cdot 10^{-2} \cdot \exp(-114,000) RT/cm^2/sec. \quad (2)$$

Let us discuss the obtained dependencies (1) and (2). First of all it is expedient to evaluate the entropy of activation  $\Delta S$  of diffusion of carbon in  $\beta$ -Zr, utilizing the well known expression:

$$D_0 = p \cdot a \cdot \nu \cdot a^2 \cdot \exp\left(\frac{\Delta S}{R}\right), \quad (3)$$

where  $D_0$  is the preexponential factor;  $p$  is the number of equivalent transpositions of interstitial atoms, equal to 4 for b. c. c. (body centered cubic);  $\nu$  is the frequency of fluctuation, equal according to evaluation  $(Q/2m \lambda^2)^{1/2}$ ;  $Q$  is the energy of activation;  $m$  is the mass of interstitial atoms;  $\lambda$  is the distance between interstitial atoms;  $a = 1/24$ ;  $a$  is the grid constant; and  $R$  is gas constant (3). For values  $D_0 = 3.6 \cdot 10^{-2} cm^2/sec$ ,  $\nu = 1.35 \cdot 10^{13} sec^{-1}$ , and  $a = 3.616 \text{ \AA}$ , we obtain the entropy of activation, equal to 4.95 cal/g-mol  $\cdot$   $^{\circ}C$ . It was not possible to compare this value with the computed one because data on temperature variation of the Young Modulus for  $\beta$  of zirconium is not known.

Table VI. Coefficients of Diffusion of Carbon in  $\beta$  of Zirconium

Conditions of Experiment		$D \cdot 10^7, cm^2/sec$
Temperature ( $^{\circ}C$ )	Duration (hr)	
1100	2	1.4
1200	5	2.2
1300	1.5	7.3
1400	4	15
1520	2	27
1600	0.5	33

Table VII. Coefficients of Diffusion of Carbon in Carbide of Zirconium

Conditions of Experiment		D, cm <sup>2</sup> /sec
Temperature (°C)	Duration (hr)	
1580	7	9.5 · 10 <sup>-12</sup>
1650	3.5	3.8 · 10 <sup>-11</sup>
1780	3	4.1 · 10 <sup>-10</sup>
1900	2	2 · 10 <sup>-9</sup>
2080	2	6 · 10 <sup>-9</sup>

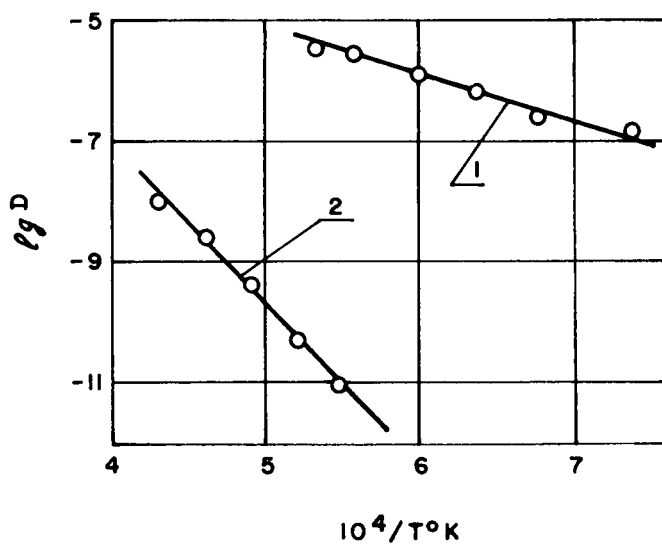


Figure 11. Temperature Dependence of Coefficients of Diffusion of Carbon in Zirconium (Equation (1)) and Carbide of Zirconium (Equation (2))

It is expedient to juxtapose the parameters of diffusion of carbon in  $\beta$  of zirconium obtained by us with analogous data for other elements of penetration (interstition). Table VIII presents these data.

Bearing in mind the correlation of Wert and Zener<sup>24</sup>,

$$\Delta S = - Q \frac{\partial(\mu/\mu_0)}{\partial T} \quad , \quad (4)$$

where  $\mu$  and  $\mu_0$  are modulus change at a given temperature and 0°K, it is evident that the relation of entropy of activation to energy of activation should be constant for the diffusion of various interstitial elements into the same metal. For convenience, this relation ( $\Delta S/Q$ ) is usually multiplied by  $T_{PL}$  and a dimensionless parameter is obtained<sup>25</sup>, characterizing the temperature variation of the shift module.

$$\beta = \frac{\Delta S}{Q} T_{PL} = \frac{\partial (\mu/\mu_0)}{\partial (T/T_{PL})} \quad (5)$$

Expressions (4) and (5) assume the absence of relaxation which, of course, is only the first approximation.

Table VIII presents values of  $\Delta S$  and  $\beta$  computed by us according to other data<sup>26,27,28,29</sup>. As it is apparent from presented results, values  $\beta$  for diffusion of hydrogen, nitrogen, oxygen, and carbon in zirconium have basically the same order. The concurrence of results for oxygen, nitrogen, and carbon are relatively good, but somewhat poorer for hydrogen. In absolute magnitude, the values evaluated by us had a meaningful character. Thus for other metals, the b. c. c. parameter  $\beta$ , determined from direct measurements of temperature dependence of the module change, comprises, for example, 0.43 for  $\alpha$  iron and 0.40 for tantalum<sup>30</sup>.

Analysis of the results of Table VIII thus shows that the parameters of diffusion of various interstitial elements into  $\beta$  of zirconium are juxtapositional.

In the investigation of diffusion of interstitial elements, it is common practice to use a model of "touching hard spheres"<sup>31,32,33</sup>. In work by Schumann<sup>31</sup>, attention was directed to the fact that the energy of the activation of diffusion of hydrogen, nitrogen, and carbon in  $\alpha$  iron is dependent linearly on the radii of these two elements, and, furthermore, the "zero" energy of activation corresponded to the dimension of the octahedral pore.

An analogous dependence was observed as well for diffusion of interstitial elements into  $\beta$  of zirconium (Figure 12). The atomic radii  $r_H = 0.36$ ,  $r_O = 0.6$ ,  $r_N = 0.70$ , and  $r_C = 0.77$  Å are taken from other works<sup>13,14,15</sup> and relate to covalent radii.

It is characteristic that the value of the radius, corresponding to the "zero" value of activation energy, comprises about 0.25 Å which is very similar with the radius of the octahedral pores in  $\beta$  of zirconium ( $r_{OKT} = 0.24$  Å).

The first direct indications on the location of interstitial elements in the  $\beta$ -zirconium lattice are absent. As it is known, for other b. c. c. metals, the body centered cubic based on the results of internal friction and electromicroscopic investigations, the interstitial atoms are located primarily in octahedral holes<sup>16,17</sup>.

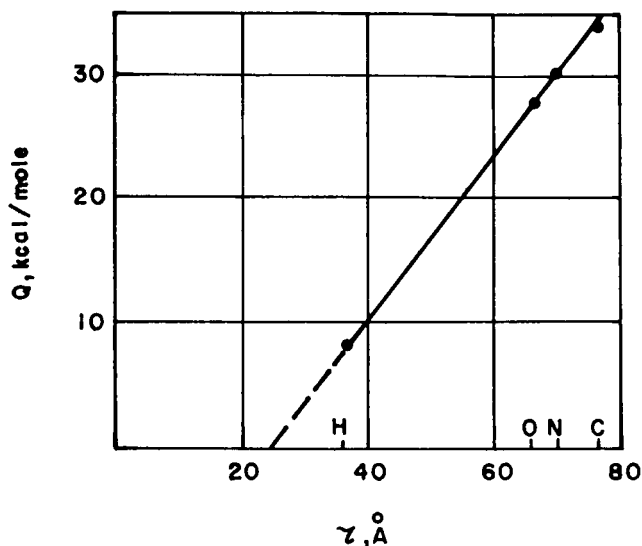


Figure 12. Dependence of Activation Energy of Interstitial Elements in  $\beta$  of Zirconium on Magnitude of Atomic Radius

For hydrogen atoms, however, a more predominant distribution in tetrahedral holes seems more natural. This is possibly explained by a higher solubility of hydrogen in  $\beta$  phases of transition metals of group IV in comparison to hexagonal  $\alpha$  phases. The dimensions of tetrahedral holes in the b. c. c. is considerably greater than in hexagonal. The estimates made by Magnier and Accary<sup>12</sup> also add evidence to the fact of predominant distribution of hydrogen atoms in tetrahedral holes of the b. c. c. of metals.

The circumstance, that regardless of possible distribution of interstitial atoms in octahedral (O) or tetrahedral (T) holes of  $\beta$ -zirconium lattice dependence  $Q = f(r)$  has a linear character, signifies that the diffusion is connected with transition through octahedral holes, i. e., it can be represented by diagrams O-O or T-O-T. From this it follows that transitions O-O, as has been noted by Magnier and Accary<sup>12</sup>, may be realized according to diagram O-T-O which, evidently, is characteristic for diffusion of carbon, nitrogen, and oxygen.

Absence of data on the modulus change for monocrystal  $\beta$  of zirconium does not permit the qualitative evaluation of the possibility of filling the tetrahedral and octahedral holes by interstitial atoms.

However, conclusions based on examination of diffusion of interstitial elements within the framework of a model of "hard spheres" are envisaged as not being unquestionable.

In such an approach, the electronic structure of solid interstitial solutions is not taken into consideration. The real value of atomic radii in solid solutions still remains unknown. Evaluations carried out according to formulas of Pauling and E. S. Sarkinson<sup>14,15</sup> indicate that the radius of a hydrogen atom may increase in solid solutions up to approximately 50 percent. The increase of atomic radii of other interstitial elements is considerably smaller (up to approximately 10-20 percent). Further investigations must refine the real character of dependence  $Q = f(r)$  and "life span" of interstitial atoms in tetrahedral and octahedral holes.

The theory of the diffusion of metallic and metalloid atoms in interstitial phases are not developed yet. Therefore, discussion of dependence (2) may be rather qualitative. Thus, it is not possible to explain the rather high significance of the preexponential factor.

In contrast to the earlier examined case of diffusion in  $\beta$  of zirconium, the diffusion of carbon in the carbide of zirconium is realized not according to the principle of interstitial but according to the principle of substitution in the metalloid sublattice of this combination. In this connection, taking into consideration as well the difference in the melting temperatures, the considerably lower diffusional mobility of carbon in the carbide of zirconium and considerably higher energy of activation, in comparison with diffusion of carbon in  $\beta$  of zirconium, seem to be absolutely natural.

Borisov, Lubov, and Temkin<sup>18</sup> made a study of the evaporation of the carbide of zirconium and established that around composition  $ZrC_{1.00}$  the evaporation occurs congruently. The value of the partial heat of sublimation  $Q$  of carbon, according to the data of this work, comprised about 178 kcal/mol.

For high melting transition metals, the relation  $Q/Q$  is usually  $0.6 \div 0.8$ <sup>19</sup>. In our case, this relation turned out to be equal to 0.65.

Bearing in mind this circumstance as well as the high melting temperature of  $ZrC$ , the obtained value of the activation energy for carbon diffusion in zirconium carbide appears to be quite reasonable.

Table III. Parameters of Diffusion of Interstitial Elements in Zirconium

Interstitial Elements	Method of Investigation	Temperature of Experiments (°C)	$D_0$ , cm <sup>2</sup> /sec	$Q$ kcal/mol	Authors	Entropy of Activation of Diffusion $\Delta S$ kcal/mol (°C)	Temperature Coefficient of Variation of Shift Module $\beta = \frac{\Delta S}{Q} \cdot T$ PL
Hydrogen		870 - 1100	$7.4 \cdot 10^{-3}$	8.5	5	0.72	0.18
		760 - 1100	$5.3 \cdot 10^{-3}$	8.3	6	0.12	0.03
Oxygen		1000 - 1500	$4.5 \cdot 10^{-2}$	28.2	7	5.9	0.44
Nitrogen		980 - 1640	$1.5 \cdot 10^{-2}$	30.7	8	3.47	0.24
Carbon	Isotope	1100 - 1600	$3.6 \cdot 10^{-2}$	34.2	Published Works	4.95	0.31

## LITERATURE CITED

1. V. Zeit, DIFFUSION IN METALS, Foreign Literature Publication, M. 1958.
2. R. Sh. Malkovich, F. M. M., 15, No. 6, 880 (1963).
3. R. Kieffer and Benesovsky, CARBIDES IN HARD MATERIALS, Springer-Verlag, Vienna, 44-266 (1963).
4. W. A. Frad, CARBIDES, IS 722 (1963).
5. G. V. Samsonov, HIGH MELTING COMBINATIONS, GNTL., M., (1963).
6. P. V. Gel'D and A. P. Lubimov, Reports of Academy of Sciences, OTN, No. 6, 119 (1961).
7. G. V. Samsonov and A. P. Epik, SURFACES AND COVER FROM HIGH MELTING COMBINATIONS, Metallurgy, 41 (1964).
8. G. S. Kramer, L. D. Efros, and E. A. Voronkova, Zh T F, 22, 5, 859-873 (1952).
9. W. Chubb, C. W. Townley, and R. W. Getz, BMI, 1551 (1961).
10. G. B. Samsonov, L. V. Strashinskaya, and E. A. Shiller, Reports of Academy of Sciences, Metallurgy and Fuels, 5, 167-180 (1962).
11. S. Katz, Nuclear Materials, 6, 172, 2 (1962).
12. P. Magnier and A. Accary, Symposium on Carbides in Nuclear Energy, 5-7 November 1963, Harwell.
13. G. A. Christensen, HW 72031 (1963).
14. W. Chubb and R. F. Dickerson, American Ceram. Society Bulletin, 564-569, September 1962.
15. A. F. Weinberg and L. Jang, ADVANCED ENERGY CONVERSION, Pergamon Press, 3, 101-111 (1963).
16. C. D. Gertsriken and I. Ya. Dexter, DIFFUSION IN METALS AND ALLOYS IN SOLID PHASE, Phys-Mat-Giz, M. (1960).

17. R. Berrer, DIFFUSION IN SOLID BODIES, M. (1948).
18. V. T. Borisov, B. Ya. Lubov, and D. E. Temkin, Academy of Sciences, USSR, 104, 223-228 (1955).
19. J. A. Becker, Journal of Applied Physics, 32, 411 (1961).
20. S. Takeuchi, T. Homma, and T. Sato, Nippo Kinzoku Gakkaishi, 28 January 1964, 11-15.
21. L. N. Alexandrov and V. Ya. Shelkonogov, Powder Metallurgy, No. 4, 28-32 (1964).
22. M. Hansen and K. Anderko, STRUCTURE OF DUAL ALLOYS, T. 1. GNTL, M (1962).
23. U. F. Babikova and P. L. Grusin, METALLURGY AND PURE METALS, 2, Atomizdat, M., 1. p. 128 (1960).
24. C. Wert and C. Zener, Physical Review, 76, 1169 (1949).
25. C. Wert, Applied Physics, 21, 1196 (1950).
26. M. Someno, Journal of Japan Institute, Met., 24, 249 (1960).
27. V. Gelerunas, P. Cohn, and R. Price, Journal of Electronic Society, 110, 799 (1963).
28. M. Mallet, et. al., BMI, 1154 (1957).
29. M. Mallet, J. Belle, and B. Cleland, Journal of Electr. Society, 101, 1 (1954).
30. W. Köster and W. Rauscher, Z. Metallk., 39, 111 (1948).
31. H. Schumann, Metall Giesser Tech., 4, 305 (1954).
32. A. Ferro, Journal of Applied Physics, 28, 895 (1957).
33. D. Beshers, UCRL, 7184 (1963).
34. B. K. Weinstein, Crystallography, 33, 293 (1958).
35. L. Poling, Nature of Chemical Bonds, Cornell University Press (1962).

36. E. S. Sarkissov, ZhFKh., 37, 396 (1963).
37. K. Zinner, Ke Tin Sui, ELASTICITY AND NONELASTICITY OF METALS, IL., M. (1954).
38. J. Van Landuyt, et. al., Applied Physic Letters, 4, 15 (1964); Physica Status Solidi, 5, K1 (1964).
39. J. A. Coffmann, et. al., NP-9791, CITATION ON STORMS, E. K., Lams, 2674 (1962).

# DISTRIBUTION

	No. of Copies		No. of Copies
<u>EXTERNAL</u>		U. S. Atomic Energy Commission	1
Air University Library	1	ATTN: Reports Library, Room G-017	
ATTN: AUL3T		Washington, D. C. 20545	
Maxwell Air Force Base, Alabama 36112		U. S. Naval Research Laboratory	1
U. S. Army Electronics Proving Ground	1	ATTN: Code 2027	
ATTN: Technical Library		Washington, D. C. 20390	
Fort Huachuca, Arizona 85613		Weapons Systems Evaluation Group	1
U. S. Naval Ordnance Test Station	1	Washington, D. C. 20305	
ATTN: Technical Library, Code 753		John F. Kennedy Space Center, NASA	2
China Lake, California 93555		ATTN: KSC Library, Documents Section	
U. S. Naval Ordnance Laboratory	1	Kennedy Space Center, Florida 32899	
ATTN: Library		APGC (PGBPS-12)	1
Corona, California 91720		Eglin Air Force Base, Florida 32542	
Lawrence Radiation Laboratory	1	U. S. Army CDC Infantry Agency	1
ATTN: Technical Information Division		Fort Benning, Georgia 31905	
P. O. Box 808		Argonne National Laboratory	1
Livermore, California 94550		ATTN: Report Section	
Sandia Corporation	1	9700 South Cass Avenue	
ATTN: Technical Library		Argonne, Illinois 60440	
P. O. Box 969		U. S. Army Weapons Command	1
Livermore, California 94551		ATTN: AMSWE-RDR	
U. S. Naval Postgraduate School	1	Rock Island, Illinois 61201	
ATTN: Library		Rock Island Arsenal	1
Monterey, California 93940		ATTN: SWERI-RDI	
Electronic Warfare Laboratory, USAECOM	1	Rock Island, Illinois 61201	
Post Office Box 205		U. S. Army Cmd. & General Staff College	1
Mountain View, California 94042		ATTN: Acquisitions, Library Division	
Jet Propulsion Laboratory	2	Fort Leavenworth, Kansas 66027	
ATTN: Library (TDS)		Combined Arms Group, USACDC	1
4800 Oak Grove Drive		ATTN: Op. Res., P and P Div.	
Pasadena, California 91103		Fort Leavenworth, Kansas 66027	
U. S. Naval Missile Center	1	U. S. Army CDC Armor Agency	1
ATTN: Technical Library, Code N3022		Fort Knox, Kentucky 40121	
Point Mugu, California 93041		Michoud Assembly Facility, NASA	1
U. S. Army Air Defense Command	1	ATTN: Library, I-MICH-OSD	
ATTN: ADSX		P. O. Box 29300	
Ent Air Force Base, Colorado 80912		New Orleans, Louisiana 70129	
Central Intelligence Agency	4	Aberdeen Proving Ground	1
ATTN: OCR/DD-Standard Distribution		ATTN: Technical Library, Bldg. 313	
Washington, D. C. 20505		Aberdeen Proving Ground, Maryland 21005	
Harry Diamond Laboratories	1	NASA Sci. & Tech. Information Facility	5
ATTN: Library		ATTN: Acquisitions Branch (S-AK/DL)	
Washington, D. C. 20438		P. O. Box 33	
Scientific & Tech. Information Div., NASA	1	College Park, Maryland 20740	
ATTN: ATS		U. S. Army Edgewood Arsenal	1
Washington, D. C. 20546		ATTN: Librarian, Tech. Info. Div.	
		Edgewood Arsenal, Maryland 21010	

	No. of Copies		No. of Copies
National Security Agency ATTN: C3/TDL Fort Meade, Maryland 20755	1	Brookhaven National Laboratory Technical Information Division ATTN: Classified Documents Group Upton, Long Island, New York 11973	1
Goddard Space Flight Center, NASA ATTN: Library, Documents Section Greenbelt, Maryland 20771	1	Watervliet Arsenal ATTN: SWEWV-RD Watervliet, New York 12189	1
U. S. Naval Propellant Plant ATTN: Technical Library Indian Head, Maryland 20640	1	U. S. Army Research Office (ARO-D) ATTN: CRD-AA-IP Box CM, Duke Station Durham, North Carolina 27706	1
U. S. Naval Ordnance Laboratory ATTN: Librarian, Eva Liberman Silver Spring, Maryland 20910	1	Lewis Research Center, NASA ATTN: Library 21000 Brookpark Road Cleveland, Ohio 44135	1
Air Force Cambridge Research Labs. L. G. Hanscom Field ATTN: CRMCLR/Stop 29 Bedford, Massachusetts 01730	1	Systems Engineering Group (RTD) ATTN: SEPIR Wright-Patterson Air Force Base, Ohio 45433	1
Springfield Armory ATTN: SWESP-RE Springfield, Massachusetts 01101	1	U. S. Army Artillery & Missile School ATTN: Guided Missile Department Fort Sill, Oklahoma 73503	1
U. S. Army Materials Research Agency ATTN: AMXMR-ATL Watertown, Massachusetts 02172	1	U. S. Army CDC Artillery Agency ATTN: Library Fort Sill, Oklahoma 73504	1
Strategic Air Command (OAI) Offutt Air Force Base, Nebraska 68113	1	U. S. Army War College ATTN: Library Carlisle Barracks, Pennsylvania 17013	1
Picatinny Arsenal, USAMUCOM ATTN: SMJPA-VA6 Dover, New Jersey 07801	1	U. S. Naval Air Development Center ATTN: Technical Library Johnsville, Warminster, Pennsylvania 18974	1
U. S. Army Electronics Command ATTN: AMSEL-CB Fort Monmouth, New Jersey 07703	1	Frankford Arsenal ATTN: C-2500-Library Philadelphia, Pennsylvania 19137	1
Sandia Corporation ATTN: Technical Library P. O. Box 5800 Albuquerque, New Mexico 87115	1	Div. of Technical Information Ext., USAEC P. O. Box 62 Oak Ridge, Tennessee 37830	1
ORA(RRRT) Holloman Air Force Base, New Mexico 88330	1	Oak Ridge National Laboratory ATTN: Central Files P. O. Box X Oak Ridge, Tennessee 37830	1
Los Alamos Scientific Laboratory ATTN: Report Library P. O. Box 1663 Los Alamos, New Mexico 87544	1	Air Defense Agency, USACDC ATTN: Library Fort Bliss, Texas 79916	1
White Sands Missile Range ATTN: Technical Library White Sands, New Mexico 88002	1	U. S. Army Air Defense School ATTN: AKBAAS-DR-R Fort Bliss, Texas 79906	1
Rome Air Development Center (EMLAL-1) ATTN: Documents Library Griffiss Air Force Base, New York 13440	1		

	No. of Copies		No. of Copies
U. S. Army CDC Nuclear Group Fort Bliss, Texas 79916	1	<u>INTERNAL</u>	
Manned Spacecraft Center, NASA ATTN: Technical Library, Code BM6 Houston, Texas 77058	1	Headquarters U. S. Army Missile Command Redstone Arsenal, Alabama ATTN: AMSMI-D	1
Defense Documentation Center Cameron Station Alexandria, Virginia 22314	20	AMSMI-XE, Mr. Lowers	1
		AMSMI-XS, Dr. Carter	1
		AMSMI-Y	1
		AMSMI-R, Mr. McDaniel	1
		AMSMI-RAP	1
U. S. Army Research Office ATTN: STINFO Division 3045 Columbia Pike Arlington, Virginia 22204	1	AMSMI-RBLD	10
		USACDC-LnO	1
		AMSMI-RB, Mr. Croxton	1
		AMSMI-RBT	8
U. S. Naval Weapons Laboratory ATTN: Technical Library Dahlgren, Virginia 22448	1	National Aeronautics & Space Administration Marshall Space Flight Center Huntsville, Alabama	
U. S. Army Engineer Res. & Dev. Labs. ATTN: Scientific & Technical Info. Br. Fort Belvoir, Virginia 22060	2	ATTN: MS-T, Mr. Wiggins	5
		R-P&VE-MMP, Dr. Roy	1
Langley Research Center, NASA ATTN: Library, MS-185 Hampton, Virginia 23365	1		
Research Analysis Corporation ATTN: Library McLean, Virginia 22101	1		
U. S. Army Tank Automotive Center ATTN: SMOTA-RTS.1 Warren, Michigan 48090	1		
Hughes Aircraft Company Electronic Properties Information Center Florence Ave. & Teale St. Culver City, California 90230	1		
Atomics International, Div. of NAA Liquid Metals Information Center P. O. Box 309 Canoga Park, California 91305	1		
Foreign Technology Division ATTN: Library Wright-Patterson Air Force Base, Ohio 45400	1		
Clearinghouse for Federal Scientific and Technical Information U. S. Department of Commerce Springfield, Virginia 22151	1		
Foreign Science & Technology Center, USAMC ATTN: Mr. Shapiro Washington, D. C. 20315	3		
National Aeronautics & Space Administration Code USS-T (Translation Section) Washington, D. C. 20546	2		

14. KEY WORDS	LINK A		LINK B		LINK C	
	ROLE	WT	ROLE	WT	ROLE	WT
Diffusion interaction Condensates Diffusional mobility of atoms Hot cladding Unilateral single phase diffusion Diffusion equation						

UNCLASSIFIED

Security Classification

DOCUMENT CONTROL DATA - R & D

(Security classification of title, body of abstract and indexing annotation must be entered when the overall report is classified)

1. ORIGINATING ACTIVITY (Corporate author) Redstone Scientific Information Center Research and Development Directorate U. S. Army Missile Command Redstone Arsenal, Alabama 35809		2a. REPORT SECURITY CLASSIFICATION Unclassified	
		2b. GROUP N/A	
3. REPORT TITLE CONTACT DIFFUSION INTERACTION OF MATERIALS WITH CLADDING Proceedings of the Symposium on Thermodynamics with Emphasis on Nuclear Materials and Atomic Transport in Solids. Organized by the International Atomic Energy Agency, Symposium held in Vienna 22-27 July 1965. Proceedings Series, 2, 153-180 (1966)			
4. DESCRIPTIVE NOTES (Type of report and inclusive dates) Translated from the Russian			
5. AUTHOR(S) (First name, middle initial, last name) A. A. Babad - Zakhryapina			
6. REPORT DATE 19 May 1967		7a. TOTAL NO. OF PAGES 38	7b. NO. OF REFS 39
8a. CONTRACT OR GRANT NO. N/A		9a. ORIGINATOR'S REPORT NUMBER(S) RSIC-676	
b. PROJECT NO. N/A		9b. OTHER REPORT NO(S) (Any other numbers that may be assigned this report) AD _____	
c.			
d.			
10. DISTRIBUTION STATEMENT Distribution of this document is unlimited.			
11. SUPPLEMENTARY NOTES None		12. SPONSORING MILITARY ACTIVITY Same as No. 1	
13. ABSTRACT The authors consider the diffusion interaction of materials with their cladding both during fabrication in a vacuum and during protracted isothermal heating. The results are given for diffusion in the C-Zr and C-ZrC systems.			

DD FORM 1473 1 NOV 65

REPLACES DD FORM 1473, 1 JAN 64, WHICH IS OBSOLETE FOR ARMY USE.

UNCLASSIFIED Security Classification